Dynamical versus statistical downscaling for the generation of regional climate change scenarios at a Western Mediterranean basin: the Júcar River District

Vicente Chirivella, José E. Capilla and Miguel A. Pérez-Martín

ABSTRACT

Current climate change (CC) predictions for the Western Mediterranean show a significant increase in temperature, and a decrease in precipitations, with great variability depending on general circulation models (GCM) and downscaling approaches. This paper analyses how dynamic downscaling improves statistically based CC scenarios. The study area was the Júcar River Basin (JB), with results from ECHAM5 GCM, and a close time frame of 2010–2040 appropriated for decision-making. The dynamic downscaling was performed with the regional climate model (RCM) RegCM3. It was applied to a coarse grid over the Iberian Peninsula, and then to a finer grid over the JB. The RCM was customized to reproduce Western Mediterranean climatic conditions using the convective precipitation scheme of Grell; the non-convective scheme was customized by changing the default RH_{min} and C_{ptt} parameters to reproduce precipitations originated by larger-scale atmospheric circulations. The RCM results, compared to current official Spanish Agency of Meteorology (AEMET) scenarios–statistically based–reproduce much better historical data (used to verify scenarios generation). They foresee a 21.0% precipitation decrease for 2010–2040, compared to previous ECHAM4 predictions with statistical downscaling (−6.64%). The most significant reductions are in February, September and October. Average estimated temperature increase is 0.75 °C, with high increments in July (+3.05 °C) and August (+1.89 °C).

Key words | climate change, convective precipitation, downscaling, Júcar River Basin, non-convective precipitation, Western Mediterranean

Vicente Chirivella
José E. Capilla (corresponding author)
Miguel A. Pérez-Martín
Research Institute of Water and Environmental Engineering,
Universitat Politècnica de València,
Camino de Vera, s/n,
46980 Valencia,
Spain
E-mail: *jcapilla@upv.es*

INTRODUCTION

Current climate change (CC) predictions over the Mediterranean region foresee a pronounced decrease in precipitation, especially in the warm season, except for the northern Mediterranean areas in winter. The scenarios generated by the general circulation models (GCM) are generally consistent (Giorgi & Lionello 2008), although at the regional level, where predictions are obtained by downscaling methods, there are changes mainly induced by orographic conditions and other local characteristics that cannot be captured by the coarse grids used by GCM. The intensity and robustness of the CC signals produced by a range of global and regional climate models (RCMs) suggest that the Mediterranean might be an especially vulnerable region to CC.

At the most western extreme of the Mediterranean a set of CC predictions is made available by the Spanish Agency of Meteorology (AEMET 2008). These CC predictions, pursuant to the National Plan for Adaptation to Climate Change (PNACC), MIMAM (2006), are based on GCM results from the third report of the IPCC (2001), based on emissions scenarios A2, B2 and IS92a, and obtained by statistical and dynamic downscaling. The scenarios, obtained with dynamic downscaling methodologies, are part of the

doi: 10.2166/wcc.2015.207

Prediction of Regional scenarios and Uncertainties for Defining EuropeaN Climate change risks and Effects, EU 5th Framework (PRUDENCE) project (Hesselbjerg & Bøssing 2005), and only provide results for the last third of the 21st century. In this project, local boundary conditions for RCMs are taken from the general circulation model HadCM3 (Rodríguez Diaz *et al.* 2007) and ECHAM4, which are considered the circulation models that best reproduce European climate conditions. ECHAM4 is a release of the ECHAM model series (Roeckner *et al.* 1996).

The scope of the research presented in this paper for future CC scenarios is the period 2010–2040. This is a time frame that is easier for policymakers to understand, and is much closer than most predictions, which address the end of the century. Decision-makers in charge of water resources planning need to count on reliable estimates of CC impacts (Tanaka *et al.* 2006) for a reasonable time term. Thus, most projections, generally obtained for the end of this century, are not really useful for planning. This is unrealistic considering the possibility of making decisions that might strongly affect many socio-economic aspects, based on model predictions 80 years ahead.

There are eleven AEMET scenarios for this period, and all of them have been generated by statistical downscaling. A more detailed description is presented by Chirivella (2011). Every scenario includes the historical period 1960–1990, referred to as the control period, where historical records are available and can be compared to simulated scenarios, as will be recalled below. Statistical downscaling techniques are based on quantitative relationships between atmospheric variables (predictors) and local surface variables (predictands) (Wigley 2004). This approach is based on the assumption that the relationships established among predictors and predictands remain invariant in the future, even under the CC scenario. This is clearly questionable and future research will certainly address the validity of this assumption. The statistical methods that have been used to generate the AEMET scenarios include two approaches. The first, the Statistical Downscaling Method (Wilby *et al.* 2002), is based on regression models of temperature and precipitation at weather stations, and every predictand (precipitation, maximum temperature and minimum temperature). The second, the Analogues Method, is based on calibrating relationships among predictors and predictands but considers only observed data on days, time periods, or events in which the patterns of atmospheric circulation show a certain degree of similarity. Thus, large-scale situations simulated by the GCM are used to find similar situations within the historical records database. The set of similar observed situations leads to a calibrated relationship that is used for the downscaling process.

Schmidli *et al.* (2007) compared results of different statistical downscaling models and RCM in the European Alps. They found that statistical methods strongly underestimate the magnitude of the year-to-year variations and that the RCM are more capable of reproducing spatial variability over complex terrains. More recently, Jang & Kavvas (2015) compared statistical downscaling results with an RCM for northern California, finding clearly better results with the RCM and concluding that it is questionable whether the statistical method applied is suitable for the assessment of the impact of future CC at regional scales as the future climate will evolve in time and space as a nonlinear system with land–atmosphere feedbacks. The Western Mediterranean, and more specifically the Spanish Mediterranean, can be subjected to different climatic influences with important changes from the coast to inland areas. Thus, for the region of Valencia, according to Millan *et al.* (2005), the precipitation components include Atlantic fronts, convective–orographic storms, and easterly advections over the Mediterranean Sea, all of which define the trends and changes of the temporal and spatial variability of precipitation. It is questionable whether current statistical methods can properly reproduce the local combination of these components together with the influence of short-distance orographic variability in this area. These circumstances call for more physically based approaches for downscaling. In this paper, the Júcar River Basin District (JB) is used as a representative example of the conditions described above. The JB is a well-studied area with a history of data collection and model applications that makes it suitable for the goals of this paper (Ferrer *et al.* 2012).

Chirivella *et al.* (2015) show that in the JB the selected AEMET scenarios reproduce historical records of temperature reasonably well (with average differences between -1.53 and $+1.88$ °C, and a total average of -0.05 °C). However, they underestimate the precipitation (with an average value 20% lower than observations in the control period:

1960–1990), and have a large dispersion (with deviations ranging from −28.42 to −7.53%). Moreover, the spatial and temporal dispersion of precipitation distributions, in every scenario, is also noticeable within the control period. As shown by Chirivella *et al.* (2012, 2015), differences between future and past climate remain within the range of precipitation anomalies, as represented by the simulated series provided in every CC scenario (see Mizanur *et al.* 2007; Rodríguez Diaz *et al.* 2007), and this could have a direct impact on the future availability of water resources in the basin. These authors also show that scenarios based on ECHAM4 results, four out of the eleven scenarios, are the most consistent among them, compared to the dispersion found when using other GCM. ECHAM4 also reproduces the precipitation in the upper basin better than the other models, even when examining more recent records (Ferrer Polo 2009). These facts support, although they are subject to future scientific evidence, the robustness of the ECHAM4 model to be used in this study area. It is also important to know that according to Chirivella *et al.* (2015) CC scenarios based on ECHAM4 predict a decrease of available water resources of 10% within the period 2010–2014. However, these scenarios do not reproduce the spatial distribution of temperature and precipitation well enough during the control period.

Given the differences between the simulated values of precipitation and temperature variables with historical records in the control period, there is a need to look for more accurate and appropriate methods to generate new regionalized scenarios in the area, and dynamic downscaling is considered a potential alternative. In addition, new scenarios can be based on the results of GCM from the fourth report of IPCC (2007), which are expected to be more reliable and accurate than those used in the regionalized scenarios released by AEMET in 2008 (based on the third report of the IPCC 2001). The robustness shown by the model ECHAM4 in the study area is an important reason to use this model, and its newer versions, as the basis for the generation of new regionalized scenarios.

Based on the above considerations, the research described in this paper explores – for the first time – the application of dynamical downscaling methods to generate short-term (2010–2040) scenarios and compares them to current available scenarios based on statistical methods. As a starting point we used ECHAM5 GCM results (Roeckner *et al.* 2003) described in the fourth report of IPCC (2007), and the emissions scenario A1B (Nakicenovic & Swart 2000). The RCM used is RegCM3, version 3.1 (Elguindi *et al.* 2007). RegCM3 is a well-known and validated RCM that has been successfully applied in different geographical regions all over the world, including the Iberian Peninsula (IP). It provides a representation of precipitation physics that is adequate for the Western Mediterranean area, allowing the customization of some basic parameters. Moreover, it is a user-friendly, open source and multiple platform model; these facts facilitate the transmission of its application to other researchers and an easy reproduction of the simulations. This model is the third generation of the RCM originally developed at the National Center for Atmospheric Research during the late 1980s and early 1990s. The model is currently supported by the Abdus Salam International Centre for Theoretical Physics (ICTP), Trieste, Italy. The model application presented in this paper requires both a progressive downscaling of ECHAM5 results, and the customization of the RCM. The first is done by applying RegCM3 to a coarse grid over the IP. Then, a finer grid nested in the previous one supports its application to the JB area. At the same time, in order to reproduce the specific climatic characteristics, RegCM3 parameters are customized using the period 1990–2000 as the control period. Thus, both convective precipitation and non-convective precipitation schemes are analysed in order to better fit historical records. We show comparisons of how the dynamical approach improves the reproduction of control periods with respect to previous statistical scenarios, and the change in temperature and precipitation predictions.

THE JÚCAR RIVER BASIN DISTRICT

The Júcar River Basin District, located in Eastern Spain, extends over 43,000 km^2 and is made up of three main rivers called the Júcar, the Turia and the Mijares, and by other minor watersheds, all discharging into the Mediterranean Sea. Most of the JB's territory belongs to the region of Valencia (Figure 1) with some areas in the neighbouring regions of Aragon, Catalonia and Castilla-La Mancha. Thus, water planning and management depend on the

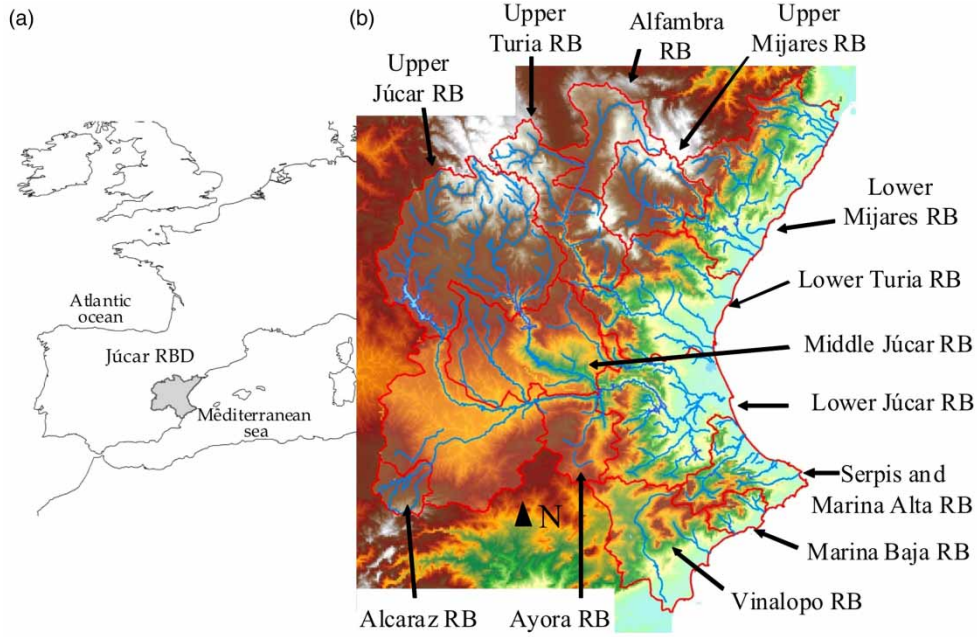

Figure 1 | Júcar River Basin: (a) geographical location and (b) the three main rivers, Júcar, Turia and Mijares, and hydroclimatic zones.

Spanish government through the Júcar River Basin Authority (*Confederación Hidrográfica del Júcar*).

The climate in the JB has a high temporal and spatial variability, with an average annual rainfall of 500 mm, varying between 320 mm/year for the driest years to 800 mm/year in the wettest years. The average annual rainfall in turn has important spatial differences; in southern areas the average annual rainfall stands at values lower than 300 mm, while in other areas it reaches values above 800 mm. Within the geographical scope of the JB we can distinguish several hydroclimatic areas (Pajares & Ferrer Polo 2002), shown in Figure 1.

METHODOLOGY

The steps followed in this research include: the customization and application of RegCM3 over the IP and the JB areas, the comparison of dynamically obtained results with statistically based previous results with the respective control periods, and the comparison of predictions for future CC. As explained above, we started with the ECHAM5 GCM results, which were processed to be dynamically downscaled with the RCM RegCM3. This model has been extensively used in several studies (e.g. Kieu *et al.* 2005, 2006; Mizanur *et al.* 2007; Zanis *et al.* 2009). The model is made up of three modules: Pre-processing, Process, and Post-process. Pre-processing includes, in turn, two steps: Terrain and ICBC. Terrain defines the domain and mesh size (10 km is the minimum value available), and interpolates the land use and geometric dimensions at each point of the grid (2 minutes is the maximum resolution data). ICBC integrates climate data from the GCM models and incorporates them into the grid. These data are the initial and boundary conditions during simulation. The Process module solves the equations of the dynamic model at the spatial mesh defined. Finally, Post-processing obtains monthly and annual averages of climate variables.

The downscaling process has been developed in two steps, as illustrated in Figure 2. Note that the resolution of the model over the JB area goes from roughly four cells, in ECHAM5, to 35×34 cells in the RegCM3 nested grid. The customization of RegCM3 for the JB area included the adjustment of the convective and non-convective precipitation schemes by calibrating the parameters that the RCM provides for this purpose. This is a process usually necessary to adapt the model capabilities to the climatic characteristics of the area under study, see for instance Davis *et al.*

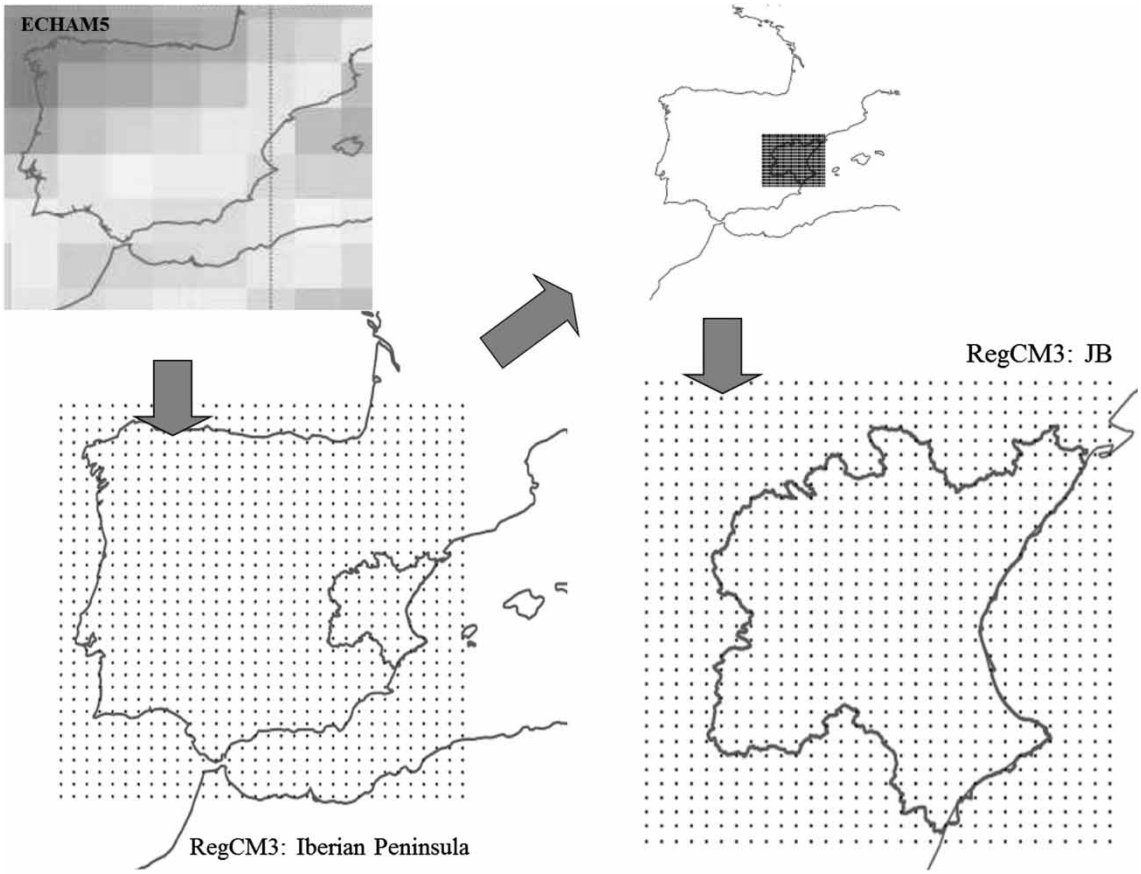

Figure 2 | Dynamic downscaling from ECHAM5 GCM. On the left, the first step: application to the IP with a regular coarse grid of 30 × 30 km. On the right, the second step: application to the JB area, using a finer grid of 10 × 10 km nested in the coarse grid.

(2009). The process followed to customize the RCM for the studied basin takes into account that this area is subjected to the combined influenced of convective and non-convective precipitations, but convective precipitations provide the greater amount of rainfall. Moreover, the boundary conditions obtained from the GCM (ECHAM5) determine when and where these mechanisms appear. This latter fact also conditions the relative independence in the results of the RCM when adjusting the convective and non-convective precipitation modules of the model. Thus, we have proceeded with a prior analysis of the applicable convective schemes available in RegCM3, and then with a lower-order adjustment using the customization of the non-convective scheme.

Following the above procedure, four different simulations were performed for every grid in order to analyse the results of the four convective precipitation schemes available in the RCM: the Kuo scheme (Anthes 1977) (referred to as simulation KS in this paper), the Grell scheme AS74 (Arakawa & Schubert 1974) (simulation GSA), the Grell scheme BC80 (Fritsch & Chappell 1980) (simulation GSB), and the Emanuel scheme (Emanuel & Zivkovic-Rothman 1999) (simulation ES). These convective precipitation schemes are designed to account for the vertical transport of latent heat, and to reduce thermodynamic instability so that the grid-scale precipitation and cloud parameterization schemes do not create unrealistic large-scale convection and overly active low-level cyclogenesis. Thus, convective schemes reduce instability by rearranging temperature and moisture in a grid column. Some schemes work well for some situations and geographical areas, and poorly for others. When compared to the Kuo scheme, the

Grell scheme is complex. It includes the effects of moisture detrainment from convective clouds, warming from environmental subsidence, and convective stabilization in balance with the large-scale destabilization rate. According to *Peng et al. (2004)*, the Emanuel scheme shows some weaknesses including a warm bias at upper levels, a weak wind bias at all levels, and under prediction of heavy-precipitation events. Although these considerations might directly lead to selecting the Grell scheme, this paper includes the analysis of simulations with the different schemes. Comparing these four simulations with the historical records in the control period 1990–2000, we have chosen the one that best reproduces the average temperature variables (mean maximum and minimum temperature) and the cumulative monthly rainfall. This comparison has been made for the whole JB, and for each hydro climatic area shown in Figure 1. After the selection of the convective precipitation scheme, the non-convective precipitation scheme has been adjusted to improve the reproduction of winter precipitation historical records.

CUSTOMIZATION OF THE REGIONAL CLIMATE MODEL AND RESULTS

Convective precipitation scheme

Table 1 and Figure 3 show both the average of monthly precipitation (P) and temperature (T) in the JB for the period 1990–2000, and both historical and simulated P and T values for the nested grid obtained with each convective precipitation scheme.

Table 1 | Average monthly precipitation (mm) and temperature (°C) for the control period (1990–2000): historical records and simulated values with the four convective precipitation schemes

		RegCM3 P (mm) simulated values					RegCM3 T (°C) simulated values			
	Historical records P	GSB	GSA	ES	KS	Historical records T	GSB	GSA	ES	KS
October	66.12	71.75	77.75	107.20	90.56	14.56	15.74	14.92	15.81	15.39
November	34.54	43.71	49.51	48.37	86.86	10.24	10.40	10.22	10.68	10.03
December	51.47	22.73	30.89	19.81	32.61	7.42	8.22	7.92	8.44	7.74
O-N-D	152.14	138.20	158.14	175.38	210.03	10.74	11.46	11.02	11.64	11.06
January	40.11	40.02	41.37	45.41	46.48	6.44	6.96	6.80	7.22	6.58
February	32.32	70.26	61.64	78.20	73.84	7.88	7.28	7.53	7.60	7.23
March	31.28	29.51	38.24	46.79	41.16	10.55	8.55	8.52	8.56	8.25
J-F-M	103.71	139.80	141.25	170.41	161.47	8.29	7.60	7.62	7.79	7.35
April	39.11	34.09	34.90	64.78	39.44	12.04	12.57	12.15	12.40	11.87
May	44.84	29.63	29.00	62.74	42.97	15.92	15.53	15.56	15.32	15.32
June	29.65	20.50	16.45	43.49	13.36	20.12	21.12	20.32	20.75	20.98
A-M-J	113.60	84.21	80.35	171.01	95.77	16.03	16.40	16.01	16.16	16.06
July	13.05	24.81	22.77	54.55	10.69	23.48	23.73	22.83	23.16	23.38
August	21.55	23.04	24.55	41.13	16.93	23.94	23.48	22.46	23.18	23.62
September	47.98	52.00	54.69	83.09	55.40	19.50	19.75	19.72	19.95	19.93
J-A-S	82.57	99.85	102.01	178.77	83.01	22.31	22.32	21.67	22.10	22.31
TOTAL	**452.02**	**462.06**	**481.75**	**695.57**	**550.29**	**14.34**	**14.45**	**14.08**	**14.42**	**14.19**
Σ dif ^{2}		**2.881.89**	**2.284.20**	**9.764.99**	**5.902.54**		**8.43**	**7.56**	**2.30**	**8.01**
Seasonal Σ dif ^{2}		**2.659.24**	**2.929.18**	**17.539.78**	**7.006.18**		**1.13**	**0.93**	**1.12**	**0.98**
Max dif		**37.95**	**29.32**	**45.88**	**52.32**		**1.18**	**0.50**	**1.25**	**0.87**
Min dif		**– 28.74**	**– 20.58**	**– 31.66**	**– 18.86**		**– 1.99**	**– 2.02**	**– 1.99**	**– 2.30**

The lowest rows show the sum of squared monthly differences between the historical records and each of the simulations and other statistical criteria for comparison.

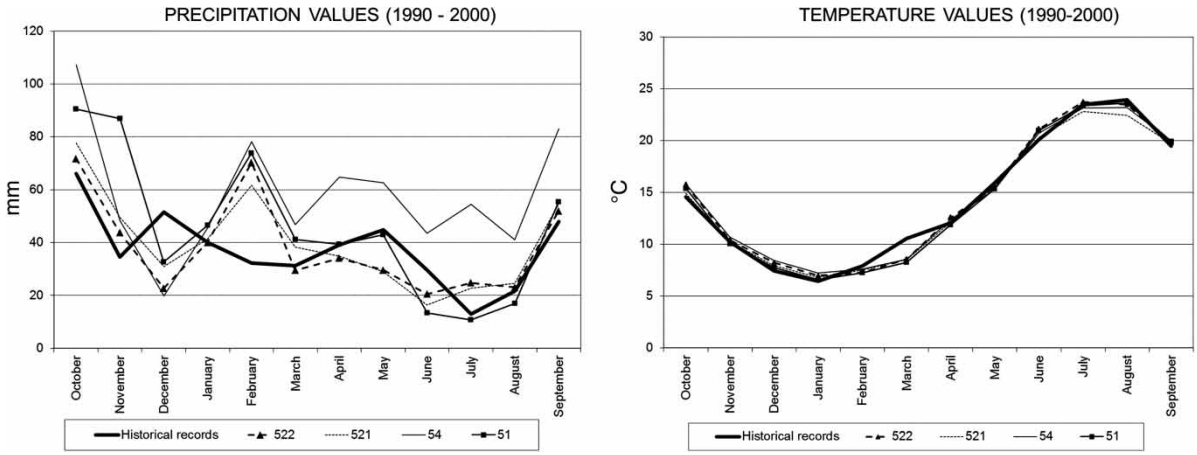

Figure 3 | Average monthly precipitation (mm) and temperature (°C) in the JB for the control period 1990–2000. Observed data and simulated values for the four convective precipitation schemes.

The four schemes correctly reproduce the temperature records, with small differences between them, and a similar behaviour in March where simulated temperature values are always slightly below the historical record. The simulations obtained with the Grell convective precipitation schemes (simulations GSA and GSB) are better than those with the Emmanuel (ES) and Kuo scheme (KS) in reproducing the historical records of precipitation, both in absolute values (462 mm/year in Grell scheme AS74; 482 mm/year in Grell scheme BC80; compared with 452 mm/year historical records), and in the sum of the squared monthly differences. Also, the simulated values with Grell schemes are closer to the historical records in autumn and winter, which is important given its influence on water resources availability (Chirivella 2011; Chirivella *et al.* 2015). Note the high value of the simulated precipitation for the month of February, which is more than two times the historical record. Simulation GSA provides the lowest value (62 mm compared to 32 mm).

The best performance of the simulations with Grell schemes can also be observed (Table 2) in most of the hydro climatic areas of JB. Simulation GSA is the closest to the particularly high rainfall recorded in the area of the Marina Alta and Serpis. Although when comparing simulations GSA and GSB the deviation of the first with respect to historical records is slightly higher (6.6%) than with the second (2.2%), GSA is selected because it approximates the precipitation much better in autumn, when convective phenomena dominate and yield one third of the annual precipitation (152.14 mm; the annual precipitation in the control period being 452.02 mm). Table 1 shows several statistical criteria to compare simulated values with historical records (monthly and seasonal sum of squared differences and maximum and minimum monthly differences). Note the clearly better behaviour of simulations GSA and GSB, as well as the fact that simulation GSA produces the narrowest difference between the maximum and minimum monthly differences shown in Table 1, for both precipitation and temperature.

Another important result that confirms the appropriateness of the RCM application for the downscaling process is that the agreement of simulated values with historical records improves from the coarse grid to the fine grid. As an illustration, Figure 4 and Table 3 show this improvement for the simulation GSA (Grell scheme AS74).

Non-convective precipitation simulation

A general problem found is that simulated scenarios yield excessive precipitation in February. The influence of larger-scale, non-convective, atmospheric circulations in the JB area (Atlantic fronts in this case study) is generally low (e.g. Estrela *et al.* 2002; Martín-Vide & López-Bustins 2006; Millán & Estrela Navarro 2008). According to our results, it seems that the non-convective precipitation scheme used in RegCM3 is not able to properly reproduce this small influence with the standard RegCM3 modelling

Table 2 | Average annual precipitation (mm) in different areas of the JB for the control period (1990–2000): historical records and simulated values for the four convective precipitation schemes

		RegCM3 simulated values			
	Historical records	**GSB**	**GSA**	**ES**	**KS**
Bajo Júcar	513.88	528,13	530.09	611.11	729.54
Alfambra	392.92	419.33	469.44	737.10	400.28
Alto Turia	448.33	478.79	525.25	786.66	548.44
Bajo Turia y Palancia	435.12	491.47	500.44	685.75	689.01
Marina Baja	442.91	264.78	267.92	441.67	266.25
Alto Mijares	479.53	557.38	589.05	954.20	537.83
Vinalopó Alacantí	295.23	260.05	255.75	359.62	241.37
Bajo Mijares	518.42	476.24	483.90	791.77	441.47
Marina Alta y Serpis	661.55	396.34	417.05	531.58	472.40
Sierra Alcaraz	473.67	384.50	398.65	567.31	342.38
Ayora Almansa	395.52	456.57	465.43	531.08	524.34
Alto Júcar	530.72	584.55	647.13	795.09	706.67
Medio Júcar	383.69	440.94	446.77	562.92	638.52
Σ (sim – histo)^2		134.002.29	149.495.76	755.428.47	329.982.40

The sum of squared differences between annual observed data and simulated values is given in the lowest row.

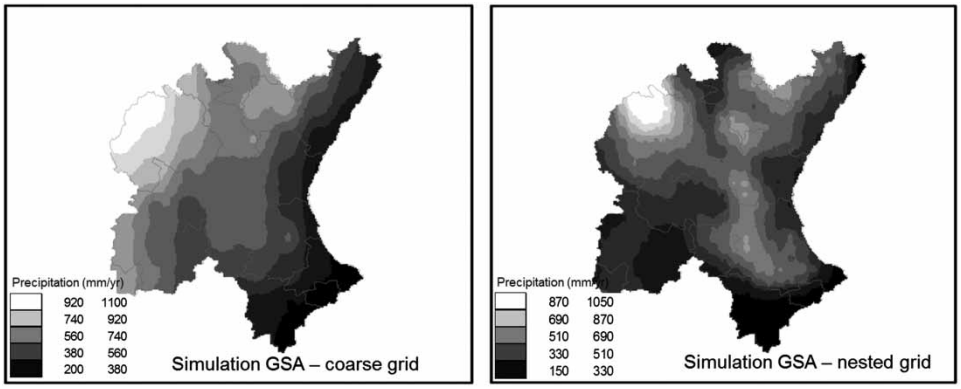

Figure 4 | Simulated annual precipitation in the period 1990–2000 (mm/yr) with Grell scheme AS74. On the left is the coarse grid and on the right the fine grid.

parameters. Non-convective precipitation is modelled by the SUBEX module (Pal *et al.* 2000) and it allows the customization of several parameters to honour local climatic conditions. SUBEX – which refers to the subgrid explicit moisture scheme – was developed to treat non-convective cloud and precipitation processes, replacing an older simple explicit moisture scheme. It calculates the autoconversion of cloud water to rainwater, accretion, evaporation, and cloud fraction at each grid point.

A careful sensitivity analysis of the influence of the different parameters on winter season precipitation was carried out. In order to do that a reduced control period of five months, November 1991–April 1992, was chosen to run RegCM3 with multiple sets of SUBEX parameters. The model was run for the whole IP using the coarse grid (Figure 2) and the Grell AS74 convective scheme already chosen. The study focused on four parameters described by Elguindi *et al.* (2007): RH_{min} which is the relative

Table 3 | Differences of average annual precipitation (mm) in the control period (1990–2000) between simulated values for the coarse grid and the fine grid and historical records, in each hydroclimatic zone of the JB

		Simulated values (ii)		$\sum$ (ii – i)^2	
	Historical records (i)	GSA (coarse grid)	GSA (fine grid)	GSA (coarse grid)	GSA (fine grid)
Upper basin					
Alfambra	392.92	638.64	469.44	10.211.98	4.610.07
Alto Turia	448.33	631.35	525.25	8.879.97	3.665.42
Alto Mijares	479.53	628.87	589.05	8.071.43	5.235.45
Sierra Alcaraz	473.67	661.30	398.65	7.992.55	3.004.44
Alto Júcar	530.72	801.79	647.13	14.868.20	6.026.23
Middle basin					
Vinalopó Alacantí	295.23	343.11	255.75	1.904.70	1.214.00
Ayora Almansa	395.52	518.53	465.43	5.013.36	2.990.16
Medio Júcar	383.69	557.18	446.77	7.125.28	3.001.48
Lower basin					
Bajo Júcar	513.88	474.58	530.09	3.944.40	4.019.22
Bajo Turia y Palancia	435.12	484.48	500.44	4.668.71	4.316.73
Marina Baja	442.91	252.25	267.92	4.427.82	3.883.15
Bajo Mijares	518.42	445.33	483.90	4.616.90	3.457.83
Marina Alta y Serpis	661.55	306.17	417.05	13.735.26	7.672.01

The sum of squared differences was obtained on a monthly basis.

humidity threshold at which clouds begin to form, C_{ppt} which can be considered as the inverse of the characteristic time for which cloud droplets are converted to raindrops, C_{evap} which is a factor that relates the percentage of precipitation that evaporates before reaching the earth's surface, and C_{aac} which is the accretion rate coefficient that correlates the amount of precipitation originated in a cell when the precipitation of the upper cells falls on it. Due to the difficulty of running RegCM3 multiple times for an automatic search of a set of parameters that yield an optimum approach to historical records, the analysis was carried out using a more simple procedure. A range of variability was defined for every parameter and the analysis of results for different subsets of modified parameters produced the best and reasonable improvement in fitting historical records. Two parameters were found to improve the reproduction of historical records: RH_{min} and C_{ppt}. Thus, RH_{min} has been increased from the default value, 0.8, given in RegCM3, to 0.9, and C_{ppt} decreased from the default value of 0.00025 to 0.0001 s^{-1}. Note that the precipitation increases when RH_{min} decreases and also when C_{ppt} increases. Finally, the results obtained with the coarse grid were verified for the fine grid in the JB domain and for more extended time periods. The fine grid even yields better simulated values in winter than the coarse grid. Thus, the simulated values for February 1992 go down to 50.77 mm/month (compared to 68.40 mm) and the total precipitation in the period of January 1992–March 1992 goes down to 109.44 mm (compared to 157.17 mm). These results are slightly better than those obtained for the coarse grid used in the sensitivity analysis.

DISCUSSION

The comparison between simulated and historical records of precipitation in the control periods shows a clear improvement for the dynamic downscaling approach obtained with the customization of RegCM3 for the JB. Figure 5 shows the difference between the control period 1960–1990 against the average of the eleven AEMET (2008) scenarios, and between the control period 1990–2000 and the

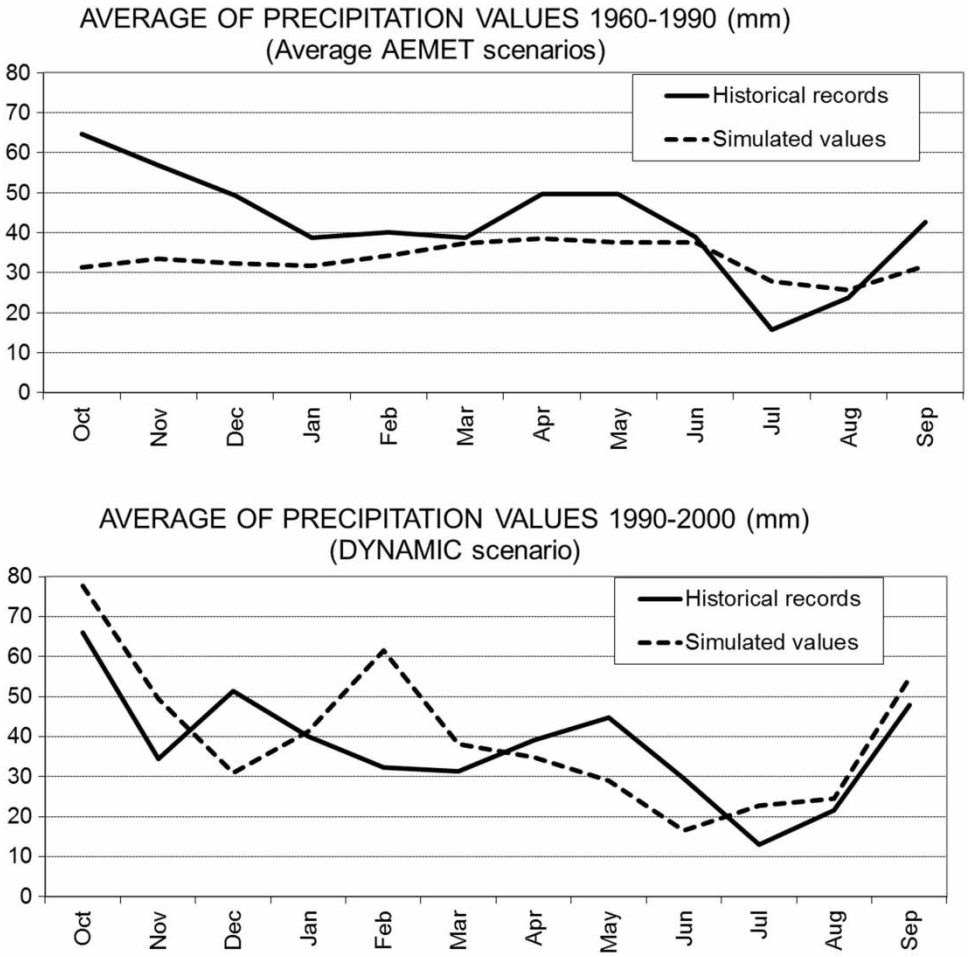

Figure 5 | Comparison between simulated and historical records of average monthly precipitation for the control periods. Upper graph for the average of AEMET scenarios and lower graph for RCM results.

RCM results. The simulated average annual precipitation in the control period of AEMET scenarios is 21% lower than the observed data, while that obtained with the new scenario is 6% higher. The latter values are shown in Table 4. In addition, the monthly distribution of precipitation obtained with RegCM3 fits the historical records better than in the AEMET scenarios (Figure 5). The sum of the square differences for the graphs in Figure 5 is 6% lower for the RegCM3 results. Moreover, if this measurement is computed without including February, then it is 41% lower. This highlights the fact that February is the only month in which the behaviour of RegCM3 is worse than for AEMET scenarios, yielding an excess of precipitation close to 30 mm (roughly 5% of annual precipitation).

Table 4 shows the detailed differences between monthly historic averages of T and P for the control period and the difference with RegCM3 simulated values (ΔT^* and ΔP^*). As indicated above, these are much closer to the control period than occurs with statistical climatic scenarios from AEMET (2008). In the same table, the climatic anomalies of T and P, ΔT and ΔP, are presented calculated for the decades 2010–2020, 2020–2030, and 2030–2040, as well as for the whole period 2010–2040. There is a clear trend of increase in T and decrease of P, with variations along the three simulated decades. For the whole territory of the JB, RegCM3 foresees a 21.0% decrease in precipitation for the period 2010–2040, i.e., 95.23 mm/year. This is considerably greater than the average anomaly predicted by the average

Table 4 | Differences of simulated T and P with the control period, ΔT* and ΔP*, and anomalies of T and P, ΔT and ΔP, for the decades 2010–2020, 2020–2030 and 2030–2040, and for 2010–2040, referred to the control period 1990–2000

	1990–00 observed data		1990–00 RegCM3		2010–20		2020–30		2030–40		2010–40	
	T	P	ΔT*	ΔP*	ΔT	ΔP	ΔT	ΔP	ΔT	ΔP	ΔT	ΔP
October	15.03	66,12	−0.11	11.63	−0.65	−29.75	0.33	−40.93	0.30	−21.98	−0.01	−30.89
November	10.06	34.54	0.16	14.97	−0.11	−8.51	0.12	−21.12	0.65	−12.06	0.22	−13.90
December	7.15	51.47	0.77	−20.58	−0.68	22.58	−0.10	0.78	0.12	3.55	−0.22	8.97
O–N–D	10.75	152.14	0.27	6.01	−0.48	−15.68	0.12	−61.27	0.36	−30.49	0.00	−35.81
January	6.50	40.11	0.31	1.26	−0.09	−3.87	0.47	−0.89	−0.16	−3.41	0.07	−2.72
February	7.63	32.32	−0.09	29.32	0.40	−33.31	−0.56	−26.85	1.50	−30.50	0.45	−30.22
March	10.34	31.28	−1.82	6.96	0.76	−10.75	0.26	−10.42	0.34	15.30	0.45	−1.96
J–F–M	8.16	103.71	−0.54	37.54	0.36	−47.93	0.06	−38.16	0.56	−18.61	0.32	−34.90
April	12.20	39.11	−0.05	−4.21	1.22	0.29	−0.20	−10.12	0.51	−7.75	0.51	−5.86
May	15.97	44.84	−0.41	−15.84	0.77	7.02	1.35	−16.11	0.68	−2.28	0.93	−3.79
June	20.62	29.65	−0.29	−13.20	0.93	6.08	0.83	5.16	1.83	18.98	1.20	10.07
A–M–J	16.26	113.60	−0.25	−33.25	0.97	13.39	0.66	−21.07	1.01	8.95	0.88	0.42
July	23.72	13.05	−0.89	9.72	2.05	−6.28	2.24	−6.78	4.86	−2.75	3.05	−5.27
August	23.81	21.55	−1.35	3.00	1.33	−2.94	1.65	4.73	2.68	−0.02	1.89	0.59
September	19.59	47.98	0.14	6.71	0.27	−26.72	−1.07	−11.72	2.21	−22.33	0.47	−20.26
J–A–S	22.37	82.57	−0.70	19.44	1.22	−35.94	0.94	−13.77	3.25	−25.10	1.80	−24.94
TOTAL	**14.38**	**452.02**	**−0.30**	**29.74**	**0.52**	**−86.16**	**0.44**	**−134.27**	**1.29**	**−65.25**	**0.75**	**−95.23**

of statistically based AEMET scenarios, −4.03%, and −6.64% predicted by the average of scenarios based on ECHAM4 (Chirivella *et al.* 2015). The most significant reductions are produced in the months of February, September and October. The increase in average temperatures is estimated as 0.75 °C, from a simulated value of 14.08 °C in the decade 1990–2000, to an average of 14.83 °C for 2010–2040. Note that this increment is strongly concentrated in the summer months: in July (+3.05 °C) and in August (+1.89 °C).

It is important to understand the influence that the temporal and spatial distribution of anomalies will have on the availability of water resources (Bates *et al.* 2008). The impact on water resources also depends on seasonal and spatial variations of T and P. According to the results of the RCM, the greatest reductions of P, in percentage terms, are expected in coastal areas, being less pronounced in inland areas; this change is more pronounced in autumn and winter, thus foreseeing a greater impact on water resources. Regarding T, the increase in absolute value (not in percentage) is similar at upper-, mid- and lower-basin areas. As already indicated above, its increment is mainly concentrated in the summer months, reducing its adverse effect on water resource availability, but posing a serious threat regarding potential future heat waves.

Another interesting result seen when comparing with statistically-based AEMET predictions, is that the RegCM3 anomaly precipitation variation during the three decades (−86.16, −134.27, −65.25 mm) is much higher than that obtained by the AEMET scenarios (−5.46, −12.73, −19.55 mm), while maintaining a decreasing trend. The same results are observed with respect to spatial variability (Chirivella *et al.* 2015). This confirms the results obtained by Schmidli *et al.* (2007) when comparing downscaling methodologies in a different regional environment.

The RCM projections shown in this paper show trends similar to those generated in the ENSEMBLES project (Van der Linden & Mitchell 2009), although in this project there are different downscaling approaches, applied to different regional studies, and for the end of the 21st century. In ENSEMBLES, some scenarios predict P anomalies close to −20% and a T anomaly of 1 °C in some parts of Spain. These

results are also based on the fourth report (AR4) of IPCC, and A1B emissions scenarios, although they refer to a longer time period.

CONCLUSIONS

This paper presents the results of a dynamical downscaling approach compared to others obtained by statistical methodologies. The geographical area where the study was carried out is a Western Mediterranean basin, the Júcar River Basin (JB), where there is a combined influence, over short distances, of precipitations of different origin (convective and non-convective precipitations), together with strong impact from local orography variability. The time frame was the period 2010–2040, for which no previous dynamic scenarios have been generated and only statistical ones are available.

The RCM used, RegCM3, was applied using a coarse grid of 30×30 km over the IP, and then a nested grid of 10×10 km was applied over the JB area. The starting input data came from the ECHAM5 GCM model (fourth report of IPCC). Thus, the resolution over the JB goes roughly from four cells (ECHAM5) to 35×34 cells (RegCM3 with a fine grid). The RCM was successfully customized to reproduce the local convective and non-convective precipitations and local conditions. The most suitable convective scheme was found to be the Grell scheme AS74 (Arakawa & Schubert 1974). The non-convective scheme was adapted by changing some of the default RegCM3 parameters (RH_{min} and C_{ppt}) in order to diminish the influence of Atlantic fronts in the RCM results over the JB. Compared to the current official AEMET (2008) scenarios over Spain, the dynamical downscaling approach reproduces much better historical data used for the verification of RegCM3 in the control period 1990–2000.

The results of RegCM3 foresee a 21.0% decrease in precipitation in the JB for the period 2010–2040, i.e., 95.23 mm/year. This is considerably greater than previous predictions. In fact, the average of AEMET scenarios, based on ECHAM4, is −6.64% (Chirivella *et al.* 2015). The most significant reductions are produced in the months of February, September and October. Regarding temperature, the average increase is estimated to be 0.75 °C, with very significant increments in July (+3.05 °C) and August (+1.89 °C).

In short, and taking into account that this research compares statistical scenarios derived from ECHAM4 GCM against a dynamic scenario derived from ECHAM5, we conclude that statistical downscaling approaches can fail in the reproduction of local, but important, temporal and spatial climatic characteristics that have an important impact on precipitation. This fact calls for a dynamic downscaling approach that works better on a local scale, as shown in the research presented in this paper, where more recent GCM results were used. The western Mediterranean, and more specifically, the Júcar River Basin, is a good example of this situation. Moreover, the RegCM3 model has been customized for its application in the studied area for further regionalizations of CC scenarios.

ACKNOWLEDGEMENTS

We thank the Júcar District Authority for providing the data and information necessary for the research described in this paper, the Spanish Agency of Meteorology (AEMET) for the availability of historical records and future climate change scenarios, and the Abdus Salam International Centre for Theoretical Physics (ICTP, Trieste, Italy) for making available the model RegCM3 and associated data sets.

REFERENCES

AEMET 2008 *Generación de Escenarios Regionalizados de Cambio Climático para España*. Ministerio de Medio Ambiente, Medio Rural y Marino, Madrid, Spain.

Anthes, R. A. 1977 A cumulus parameterization scheme utilizing a one-dimensional cloud model. *Mont. Wea. Rev.* **105**, 270–286.

Arakawa, A. & Schubert, W. H. 1974 Interaction of a cumulus cloud ensemble with the large-scale environment, Part I. *J. Atmos. Sci.* **31**, 674–701.

Bates, B. C., Kundzewicz, Z. W., Wu, S. & Palutikof, J. P. (eds) 2008 *Climate Change and Water*. Technical Paper of the Intergovernmental Panel on Climate Change. IPCC Secretariat, Geneva, 210 pp.

Chirivella Osma, V. 2011 *Characterization of Future Climate Scenarios in the Valencian Community: Suggestions for Improvements to the Assessment of Water Resources Supply*

and Demand. PhD Thesis, Universidad Politécnica de Valencia, Spain.

Chirivella Osma, V., Capilla Romá, J. E. & Pérez-Martín, M. A. 2012 *Regional impacts of climate change on water resources: the Jucar basin, Spain*. 2012 International Congress on Environmental Modelling and Software Society (iEMSs).

Chirivella Osma, V., Capilla Romá, J. E. & Pérez Martín, M. A. 2015 Modelling regional impacts of climate change on water resources: the Jucar Basin, Spain. *Hydrol. Sci. J.* **60** (1), 30–49.

Davis, N., Bowden, J., Semazzi, F., Xie, L. & Onol, B. 2009 Customization of RegCM3 regional climate model for Eastern Africa and a tropical Indian Ocean domain. *J. Clim.* **22**, 3595–3616.

Elguindi, N., Bi, X., Giorgi, F., Nagarajan, B., Pal, J., Solmon, F., Rauscher, S. & Zakey, A. 2007 *RegCM Version 3.1: User's Guide*. Abdus Salam International Centre for Theoretical Physics (ICTP), Trieste, Italy. http://users.ictp.it/RegCNET/regcm.pdf (accessed 26 March 2015).

Emanuel, K. A. & Zivkovic-Rothman, M. 1999 Development and evaluation of a convection scheme for use in climate models. *J. Atmos. Sci.* **56**, 1766–1782.

Estrela Navarro, M. J., Pastor, F. & Millán, M. M. 2002 Air mass change along trajectories in the western Mediterranean basin in the torrential rains events in the Valencia Region. In: *Proceedings of the 4th EGS Pinius Conference*. Mallorca, Spain.

Ferrer, J., Pérez-Martín, M. A., Jiménez, S., Estrela, T. & Andreu, J. 2012 GIS-based models for water quantity and quality assessment in the Júcar River Basin, Spain, including climate change effects. *Sci. Total Environ.* **440**, 42–59.

Ferrer Polo, J. 2009 Mainstreaming climate change scenarios in the analysis of the Water Plans. Application to the Jucar river. In: *Communication Presented at Conference 'Climate Change Impacts in the Planning and Management of Water Resources'*. 1 December, Valencia, Spain.

Fritsch, J. M. & Chappell, C. F. 1980 Numerical prediction of convectively driven mesoscale pressure systems. part I: convective parameterization. *J. Atmos. Sci.* **37**, 1722–1733.

Giorgi, F. & Lionello, P. 2008 Climate change projections for the Mediterranean region. *Glob. Planet. Change* **63** (2–3), 90–104.

Hesselbjerg Christensen, J. & Bøssing Christensen, O. 2005 A summary of the PRUDENCE model projections of changes in European climate by the end of this century. *Clim. Change* **81**, 7–30.

IPCC 2001 Climate change 2001: the scientific basis. In: *Contribution of Working Group I to the Third Assessment Report of the Intergovernmental Panel on Climate Change* (J. T. Houghton, Y. Ding, D. J. Griggs, M. Noguer, P. J. van der Linden, X. Dai, K. Maskell & C. A. Johnson, eds). Cambridge University Press, Cambridge, NY, USA, 881 pp.

IPCC, and 2007 Climate change 2007: synthesis report. In: *Contribution of Working Groups I, II and III to the Fourth Assessment Report of the Intergovernmental Panel on Climate Change* (Core Writing Team, R. K. Pachauri & A. Reisinger, eds). IPCC, Geneva, Switzerland, 104 pp.

Jang, S. & Kavvas, M. 2015 Downscaling global climate simulations to regional scales: statistical downscaling versus dynamical downscaling. *J. Hydrol. Eng.* **20** (special issue: Grand Challenges in Hydrology), A4014006.

Kieu, T. K., Duc, L. & Minh, H. T. H. 2006 *Simulation of Southeast Asia Rainfall using RegCM3 and Problems*. Vietnam National University of Hanoi, Vietnam. http://www.hyarc.nagoya-u.ac.jp/game/6thconf/html/abs_html/pdfs/T4DKTX13Aug04100242.pdf (accessed 16 December 2015).

Kieu, T. K., Minh, H. T. H. & Duc, L. 2005 *First results of seasonal simulation using RegCM3 with the Tiedtke convection Scheme for the Southeast Asia Region*. 23rd International Association of the Meteorology and Atmospheric Science (IAMAS) General Assembly Report, Beijing, China. http://web.lasg.ac.cn/IAMAS2005/download.html (accessed 17 December 2015).

Martín-Vide, J. & López-Bustins, J. A. 2006 The Western Mediterranean Oscillation and rainfall in the Iberian Peninsula. *Int. J. Climatol.* **26** (11), 1455–1475.

Millán, M. M., Estrela, M. J. & Miró, J. 2005 Rainfall components: variability and spatial distribution in a Mediterranean area (Valencia region). *J. Climate* **18**, 2682–2705.

Millán, M. M. & Estrela Navarro, M. M. 2008 Meso-Mediterranean weather, climate feedback processes and scenarios of climate change. In: *Proceedings of Meeting 'Los Riesgos Climáticos en el Mediterráneo Occidental'* (M. J. Estrela Navarro, ed.). Centro Francisco Tomás y Valiente, Valenica, Spain, pp. 29–38.

MIMAM 2006 *Ministry of Environment: Plan Nacional de adaptación al cambio climático – PNACC (National Adaptation Plan to Climate Change)*. Framework for coordination between public authorities for the activities of assessing impacts, vulnerability and adaptation to climate change. Centro de Publicaciones del Ministerio de Medio Ambiente, Madrid, Spain.

Mizanur, R., Islam, M., Uddin, A. & Afroz, R. 2007 Comparison of RegCM3 simulated meteorological parameters I Bangladesh: part II preliminary result for temperature. *Sri Lankan J. Phys.* **8**, 11–19.

Nakicenovic, N. & Swart, R. 2000 *Special Report on Emissions Scenarios: A Special Report of Working Group III of the Intergovernmental Panel on Climate Change*. Cambridge University Press, Cambridge, UK, 599 pp.

Pajares, A. & Ferrer Polo, J. 2002 Modelación cuasidistribuida de los recursos hídricos y establecimiento de zonas hidroclimáticamente afines en el ámbito de la Confederación Hidrográfica del Júcar (Quasi-distributed modelling of water resources and definition of hydroclimatic zones in the Jucar River Basin District). Thesis Degree. Universitat Politecnica de Valencia, Valencia, Spain.

Pal, J. S., Small, E. E. & Eltahir, E. A. B. 2000 Simulation of regional-scale water and energy budgets: representation of subgrid cloud and precipitation processes within RegCM. *J. Geophys. Res.* **105** (D24), 29579–29594.

Peng, M. S., Ridout, J. A. & Hogan, T. F. 2004 Recent modifications of the emanuel convective scheme in the naval

operational global atmospheric prediction system. *Mon. Wea. Rev.* **132**, 1254–1268.

Rodríguez Díaz, J. A., Weatherhead, E. K., Knox, J. W. & Camacho, E. 2007 Climate change impacts on irrigation water requirements in the Guadalquivir river basin in Spain. *Region. Environ. Change* **7**, 149–159.

Roeckner, E., Arpe, K., Bengtsson, L., Christoph, M., Claussen, M., Dümenil, L., Esch, M., Giorgetta, M., Schlese, U. & Schulzweida, U. 1996 *The Atmospheric General Circulation Model ECHAM-4: Model Description and Simulation of Present-day Climate*. Max-Planck Institute for Meteorology, Report No. 218, Hamburg, Germany, 90 pp.

Roeckner, E., Bäuml, G., Bonaventura, L., Brokopf, R., Esch, M., Giorgetta, M., Hagemann, S., Kirchner, I., Kornblueh, L., Manzini, E., Rhodin, A., Schlese, U., Schulzweida, U. & Tompkins, A. 2003 *The Atmospheric General Circulation Model ECHAM5: Part I General Description*. Report No. 349. Max Plank Institute for Meteorology, Germany.

Schmidli, J., Goodess, C. M., Frei, C., Haylock, M. R., Hundecha, Y., Ribalaygua, J. & Schmith, T. 2007 Statistical and dynamical downscaling of precipitation: an evaluation and comparison of scenarios for the European Alps. *J. Geophys. Res.* **112**, D04105.

Tanaka, S. K., Zhu, T., Lund, J. R., Howitt, R. E., Jenkins, M. W., Pulido, M. A., Tauber, M., Ritzema, R. S. & Ferreira, I. C. 2006 Climate warming and water management adaptation for California. *Clim. Change* **76** (3–4), 361–387.

Van der Linden, P. & Mitchell, J. F. B. (eds) 2009 *ENSEMBLES: Climate Change and its Impacts: Summary of Research and Results from the ENSEMBLES Project*. Met Office Hadley Centre, Exeter, UK. 160 pp.

Wigley, T. M. L. 2004 *Input needs for downscaling of climate data*. Discussion Paper. California Energy Commission. www.climatechange.ca.gov/events/2004_conference/ (accessed 25 March 2015).

Wilby, R. L., Dawson, C. W. & Barrow, E. M. 2002 SDSM–A decision support tool for the assessment of regional climate change impacts. *Environ. Model. Softw.* **17**, 145–157.

Zanis, P., Douvis, C., Kapsomenakis, I., Kioutsioukis, I., Melas, D. & Pal, J. S. 2009 A sensitivity study of the Regional Climate Model (RegCM3) to the convective scheme with emphasis in central eastern and southeastern Europe. *Theor. Appl. Climatol.* **97**, 327–337.

First received 16 August 2014; accepted in revised form 20 October 2015. Available online 27 November 2015